Journal of Electromagnetic Analysis and Applications, 2022, 14, 47-64
https://www.scirp.org/journal/jemaa
ISSN Online: 1942-0749
ISSN Print: 1942-0730

Wireless Charger Design of Robot Vacuum Cleaners with Power Repeaters for High Compatibility

Anglin Li, Dariusz Kacprzak, Aiguo Patrick Hu

Department of Electrical, Computer and Software Engineering, The University of Auckland, Auckland, New Zealand
Email: ali962@aucklanduni.ac.nz

How to cite this paper: Li, A., Kacprzak, D. and Hu, A.P. (2022) Wireless Charger Design of Robot Vacuum Cleaners with Power Repeaters for High Compatibility. *Journal of Electromagnetic Analysis and Applications*, **14**, 47-64.
https://doi.org/10.4236/jemaa.2022.145005

Received: April 24, 2022
Accepted: May 24, 2022
Published: May 27, 2022

Abstract

Curved coils constructed by flexible printed circuit board (PCB) or hand-wound Litz-wire have been steadily becoming popular due to its applicable potential on devices that have a curved body. Inductive Power Transfer (IPT) systems based on curved coils and flexible ferrite sheets may provide more flexible charging solutions for various electronic devices such as rice cookers and robot vacuum cleaners. Power repeaters are also used in IPT systems to extend wireless charging range by guiding magnetic fields to the receiving coil. The interaction of these three topics could be inspiring. In this paper, two adjustable power repeaters are applied to an IPT charging system with various curved receiving coils designed for vacuum cleaners. Two power repeaters share the identical structure as the Tx coil and could be rotated to mirror symmetrically. The input and output power are calculated by analyzing the equivalent circuit model. The self-inductance, mutual inductance, and coupling coefficient of the proposed system are obtained via finite element method simulation with variable rotating angles. Three typical IPT designs have also been simulated in ANSYS Maxwell and compared with the proposed magnetic design. The comparison indicates the enhancing feature of the passive power repeaters on coupling performance and the ability to guide the magnetic flux for better magnetic field coupling. Furthermore, two types of co-simulations defined by the power source via Simplorer are conducted to explore how much power could be transferred. The tuned system is shown to be able to provide about 32 W under 100 kHz operating frequency for charging the battery of a robot vacuum cleaner. The results from theoretical calculation and simulation align well with each other.

Keywords

Passive Power Repeaters, Inductive Power Transfer, Curved Coil,

Robot Vacuum Cleaners

1. Introduction

Since the late 19th century, when the concept of transferring power without wires was proposed by Tesla, Wireless Power Transfer (WPT) has been developed greatly from thoughts in the brain to practical applications in electronic devices, industrial equipment, electrical vehicles and many other electrical fields. Compared with transferring power through direct connections of wires and cables, wireless power transfer utilizes the interaction among the primary side, the secondary side and the alternating electromagnetic field for power delivery. The energy is transferred from the primary side to the secondary side by using the electromagnetic field. This energy transfer technique offers simplicity, portability, and safety. The near-field WPT technology could be classified as Inductive Power Transfer (IPT) or Capacitive Power Transfer (CPT). IPT has become a popular and mature technology in industrial applications like Automatic Guided Vehicle (AGV) [1], electronic devices charging [2], electrical vehicle charging [3] [4] [5] [6], biomedical implants [7] [8], lighting systems [9] [10], and many other applications.

This paper deals with the IPT technology, where the power transfer capacity is significantly influenced by the distance between the primary coil—the transmitter (Tx) and the secondary coil—the receiver (Rx). The larger the distance, the lower the power transfer could be observed. A similar effect is also caused by misalignment between the Tx and Rx. Under coil misalignment, the magnetic field leakage increases, and the lower portion of the magnetic flux is received by the Rx. In order to increase the power transferred, the magnetic flux leakage must be addressed. Several methods such as magnetic shielding [11] [12] and adding the third coil [13] [14] have been proposed to concentrate the magnetic flux and reduce the leakage of magnetic fields. Sometimes it is difficult or impractical to add an extra coil between Tx and Rx, so adding coils next to Tx becomes another choice for researchers [15]. Those added coils might passively interact with the existing magnetic field between Tx and Rx [16] [17] or could be generated by an extra circuit or power supply to produce extra magnetic fields between the original coils. Both the design and position of power repeaters may influence the distribution and direction of the original magnetic field produced by the Tx coil, so it can be used to guide and enhance the transferring range of IPT systems. For example, in [18], the power is transferred through several power repeaters which are perpendicular to the Rx step by step, and the prototype shows the ability to charge a cellphone on the top of repeaters.

IPT systems can be bulky and relatively large. In order to keep their size to the minimum, planar coils are frequently used. Planar coils could be fabricated on printed circuit boards (PCBs). The disadvantage of these planar coils is higher

eddy current loss [19] [20]. If needed, planar PCB coils [2] [21] [22] and Litz-wire coils [23] could be fabricated into curved rectangular or circular shapes, so IPT systems could be applied to more devices that have a curved body, such as rice cookers, robot vacuum cleaners or rockets with a cylindrical body. Besides, the flexible ferrite sheet could be combined with the curved coil and provides magnetic shielding. All features above raise the possibility of designing an IPT system with curved coils and power repeaters in a cylindrical cleaning appliance.

In this research, an IPT system that consists of a planar Tx coil and a curved rectangular spiral Rx coil with two adjustable passive power repeaters is proposed. The system is designated to be used with a vacuum cleaner battery. The expected power level is supposed to be higher than the rated charging power of 20 W, and the operation frequency can be 100 kHz. Two passive power repeaters are introduced to enhance the power transfer capability of the system. If needed, the power repeaters can be adjusted manually to fit various Rx coils (depending on the vacuum cleaner size). The adjustment of two power repeaters is conducted as mirror-symmetric rotating with a certain angle θ along a corner of the repeater. The coupling between Tx and Rx with different rotating angles of power repeaters was explored. A co-simulation in Ansys Maxwell was conducted to obtain the uncompensated outputs with a 20 Ω resistive load which simulates as a load. Most commercial batteries of vacuum cleaners have their own charging modules embedded inside and are compatible with multiple adapters. Those adapters could provide various direct current (DC) outputs such as 19 V - 0.6 A, 20 V - 1 A, 22.5 V - 1.25 A, and 25 V - 1 A. One typical DC output 20 V - 1 A is selected and the rated equivalent load resistance is 20 Ω in calculation and simulation. Moreover, three different structures of coil designs were compared and evaluated according to the coupling performance and power transfer performance. The proposed magnetic design was also tuned with two capacitors in series, and 32.2 W of output power is achieved with an input power of 32.6 W.

2. Proposed IPT System with Curved Coils and Power Repeaters

In Section 2, the proposed IPT system is presented from the magnetic coil design and the circuit design on both primary and secondary side.

2.1. Coil Setup

Figure 1 shows a diagram of the coil setup of a proposed IPT system for robot vacuum cleaners. The yellow cylinder represents the body of the robot vacuum cleaner. The secondary part is placed close to the inner surface of the cleaner. There is a curved rectangular coil (green) and a curved flexible ferrite (grey). The secondary circuit is set to operate with compensated network. The network consists of a tuning circuit and a rectifier to convert alternating current (AC) to DC, then provides enough power to the load. The primary side consists of a three-turn spiral coil (shown in dark orange) with flat ferrite sheets (grew) are

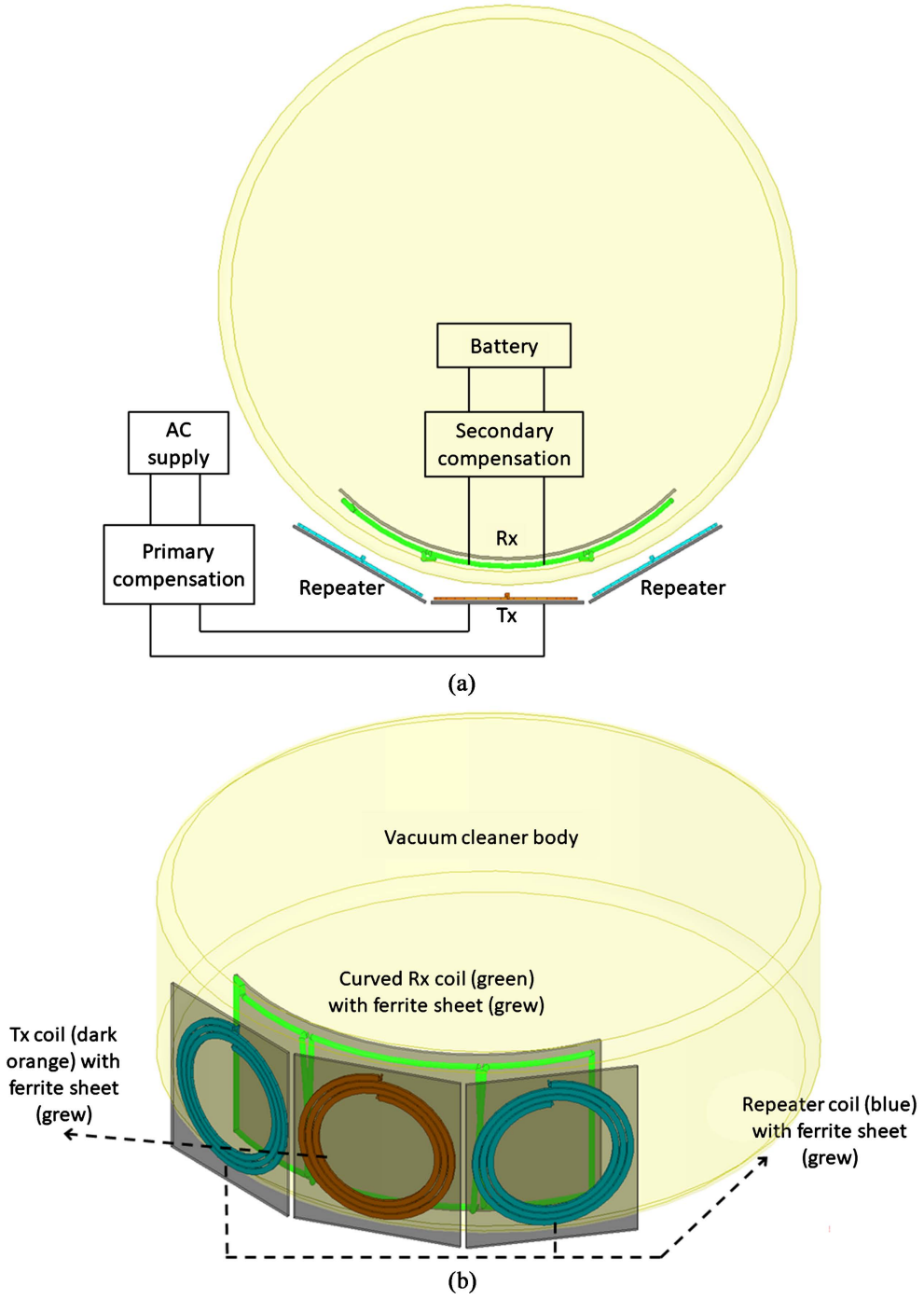

Figure 1. The Diagram of proposed coil setup with two power repeaters from (a) top view and (b)orient view. (a) The top view of the proposed system; (b) The orient view of the coil setup.

set as shown in Figure 1. The central coil and ferrite sheet works as a conventional Tx. Two passive power repeaters (blue) are placed on both sides without any excitation. The purpose of the power repeaters is to guide the magnetic flux, which allows power transfer in a case of misalignment. In this research an assumption was made that two power repeaters can be manually adjusted to fit multiple Rx coils with different curvature radius.

On the one hand, ferrite material (grew) is utilized to enhance the magnetic field. The ferrite sheets with high permeability collect and guide edge magnetic flux generated by Tx coil. It is important to mention that the flexible ferrite sheet used on the Rx side may have different characteristics compared to hard ferrite sheets used on the primary side, but both could help guide the magnetic field.

2.2. Circuit Analysis

Figure 2 shows a compensation network circuit diagram of the system for charging a robot vacuum cleaner battery. The primary side is set to operate with the mains 230 V, 50 Hz Alternating Current (AC). It is adapted to Direct Current (DC). Then the DC is converted into AC with 100 kHz for generating an alternating magnetic field. A compensation network is used to tune the operational frequency with the resonant frequency. Two power repeaters are placed in a position as shown in Figure 2. The receiver is equipped with compensation network and a rectifier. The repeater could be mirror symmetrically rotated through θ to make sure the repeater could get close to the Rx coil at an optimal angle, which could lead to a better coupling performance.

The IPT system was analyzed using the Finite Element Method. To focus on the magnetic model, the system was not powered by the mains, but by a 10 V 100 kHz sinusoidal voltage function. This is shown in Figure 3. The Tx coil and Rx coil are considered as pure inductors L_p and L_s without inner resistance, which means there is no real power loss in these inductors. Also, the inner resistance of wire and other components are neglected, so the system is close to an ideal loss free system. Two tuning capacitors C_p and C_s are added in series with L_p and L_s respectively achieve high compensation.

The value of inductance, capacitance and operating frequency satisfy following:

$$\omega_o^2 LC = 1 \tag{1}$$

The input power and output power could be obtained as:

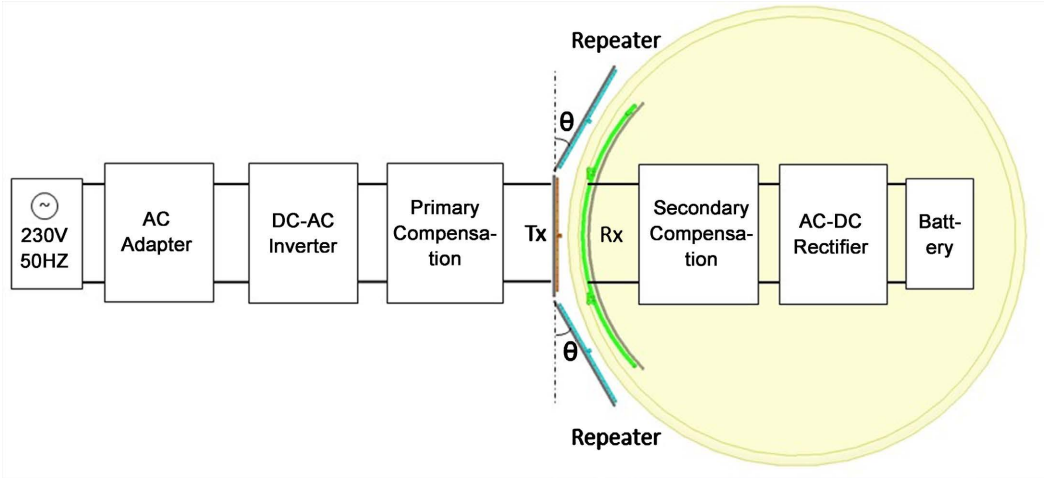

Figure 2. Circuit diagram of proposed system for battery charging.

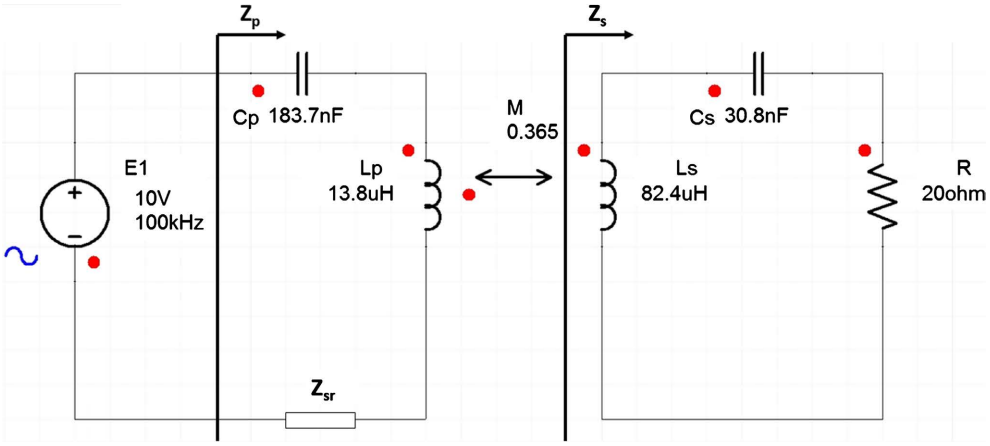

Figure 3. Equivalent circuit of the proposed system with series tuning and a 20-ohm resistive load.

$$P_{in} = I_p^2 \cdot Re\left(Z_{sr}\right) \tag{2}$$

$$P_{out} = I_s^2 \cdot R \tag{3}$$

where I_p is the primary current, I_s is the secondary current and Z_{sr} is the reflected impedance of the secondary side to the primary side.

I_p is obtained as:

$$I_p = \frac{V_{in}}{Z_p} = \frac{V_{in}}{Z_{sr} + j\omega L_p + \dfrac{1}{j\omega C_p}} \tag{4}$$

and the reflected impedance of the secondary side to the primary side Z_{sr} is:

$$Z_{sr} = \frac{\omega^2 M^2}{Z_s} \tag{5}$$

where M is the mutual inductance, Z_s is the impedance of the secondary circuit.

The impedance of the secondary side is obtained as:

$$Z_s = R + j\omega L_s + \frac{1}{j\omega C_s} \tag{6}$$

If the input current I_p is known, the output current I_p could be calculated via the loop current method:

$$j\omega L_s I_s - j\omega M I_p + \frac{I_s}{j\omega C_s} + R I_s = 0 \tag{7}$$

Table 1 shows the calculated results of the parameters mentioned above. Under series compensation condition with a rated load, the system is supposed to transfer 32.2 W power to the load. Those input and output parameters would be verified through co-simulation later and relevant comparison would be conducted.

3. Simulation Study on Coupling Performance and Power Transfer of Proposed Design

After the introduction of the magnetic design and numerical analysis of the

equivalent circuit of the proposed system, two kinds of simulation were conducted to demonstrate the magnetic coupling and power transfer capability via different software packages. In simulation study of magnetic coupling, a 3D-FEM simulation software Ansys Maxwell was used to demonstrate the magnetic design of coils with power repeaters. Model of the system is shown in Figure 4, the curvature radius of the curved Rx coil and the ferrite sheet are the same 110 mm, and the radian angle of them is 0.5π. The height of the ferrite sheet on Rx side is 64 mm. On the Tx side, the size of ferrite sheets is 58 mm × 64 mm × 1 mm and the outer radius of coils is 27.5 mm with three turns. The width of coils is 2 mm, and the thickness is 1 mm, as shown in Table 2 and Figure 4.

Table 1. Calculated results of the equivalent circuits.

Parameters	Value
Z_{sr} (Ω)	2.98 + j0.0089
Z_p (Ω)	3 + j0.33
$\dot{I}_p$ (A)	3.29 − j0.36
$\dot{I}_s$ (A)	0.06 + j1.27
I_p (A)	3.31
I_s (A)	1.27
P_{in} (W)	32.6
P_{out} (W)	32.2

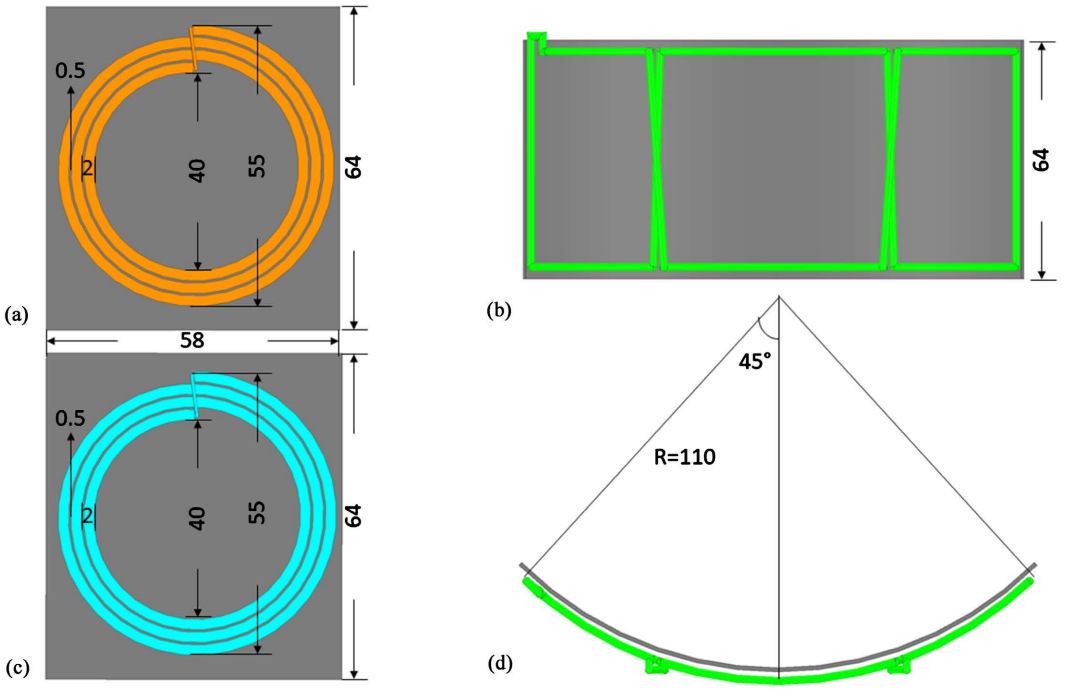

Figure 4. Geometry of (a) Tx coil, (b) Rx coil, (c) power repeaters, and (d) Rx coil.

Table 2. Specific sizes of models in Maxwell.

Coil	Setup Size
Tx outer radius (mm)	27.5
Tx inner radius (mm)	20.0
Tx width (mm)	2.0
Tx gap between turns (mm)	0.5
Tx turns	9
Rx height (mm)	64.0
Rx turns	10
Rx curvature radius (mm)	110
Rx radian angle	0.5π

In order to determine how much power could be delivered through the magnetic design, two different co-simulations involving Maxwell and Simplorer were conducted. One is the system without compensation where the Tx is with an AC current of 1 A and 100 kHz. Under this condition, the open circuit voltage V_{oc} and short circuit current I_{sc} were obtained separately. Then the output power of the uncompensated system was calculated. The other model was set to be equipped with series compensation on both sides (the primary and the secondary side), which makes the system work under fully tuned situation. The system was supplied with a 10 V 100 kHz, then input and output power was obtained from that co-simulation. The equivalent circuit of the latter co-simulation was also established and relevant parameters were calculated to be compared with the simulation results. One point that should be mentioned is the inner resistance of wire, coils and other components were ignored.

3.1. Field Distribution and Coupling Performance of Coils with Power Repeaters via Maxwell

Geometric models of the circular Tx coil with ferrite sheet, the curved rectangular Rx coil with ferrite sheet and two power repeaters with ferrite sheets are set as shown in Figure 1 and Figure 4. The air gap between the Tx coil and the Rx coil is 10 mm. A 1-amp sinusoidal current with 100 kHz is applied to the Tx coil. A typical magnetic field distribution when two power repeaters were rotated 30˚ along the neighboring edge parallel to x-axis is shown in Figure 5. It could be observed that the magnetic field distribution was symmetric. Two crossing parts of the Rx coil which was close to the neighboring edges have higher density.

Numerical results are shown in Table 3, followed by Figure 6, when power repeaters approached close to the Rx coil, self-inductance of Rx and mutual inductance between Tx and Rx presented the same rising tendency, but the coupling coefficient only went upstairs slightly. Self-inductance of the Tx coil remained stable because power repeaters might mainly influence the Rx coil in the

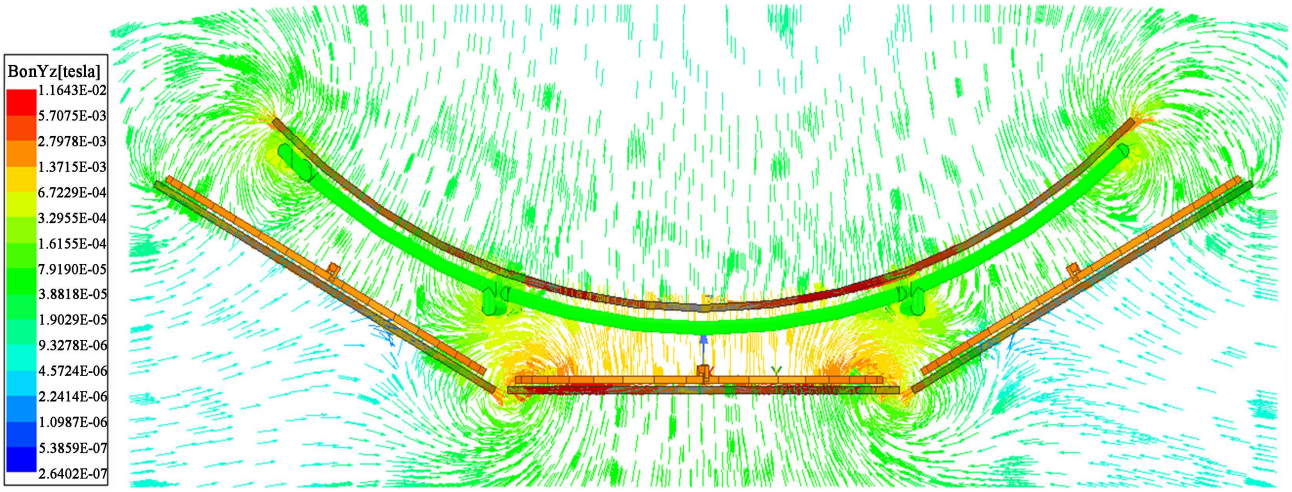

Figure 5. Magnetic flux density distribution of repeaters at 30˚.

Table 3. Self-inductance and mutual inductance between Tx and Rx under different rotating angle.

Rotating Angle (˚)	Inductance and Coupling Coefficient		
	Self-Inductance of Tx and Rx (μH)	Mutual Inductance (μH)	Coupling Coefficient
0	13.62, 76.37	11.42	0.354
10	13.66, 77.43	11.61	0.357
20	13.71, 79.10	11.88	0.360
30	13.79, 82.36	12.30	0.365
40	13.92, 90.65	13.04	0.367

system. The coupling performance between two coils was also enhanced when power repeaters were rotating closer to the Rx coil. This indicates that for a curved Rx coil with a certain curvature radius, the coupling performance with Tx coil would grow better when power repeaters get close enough to the Rx coil as possible. This adjustable feature of power repeaters could provide different curved Rx coils with the ability to achieve the best coupling state. An interesting point raised from the magnetic flux distribution of the magnetic design is that the magnetic flux lines were guided to the Rx coil by power repeaters on both right and left side. This distribution pattern could be changed to a circle pattern if the magnetic flux density on the right side distributes in opposite direction. Under this circumstance, the magnetic flux would start from center Tx coil to the left power repeater, then goes to Rx coil, next goes to the right power repeater, and finally goes back to the Tx coil. This circle running pattern of magnetic flux is similar to the distribution in an IPT system with Double-D pads, which is a popular wireless power transfer coil design. To achieve this, modifications on Tx coil and Rx coil design can be considered and power repeaters would need to have their own power supplies forming active power repeaters.

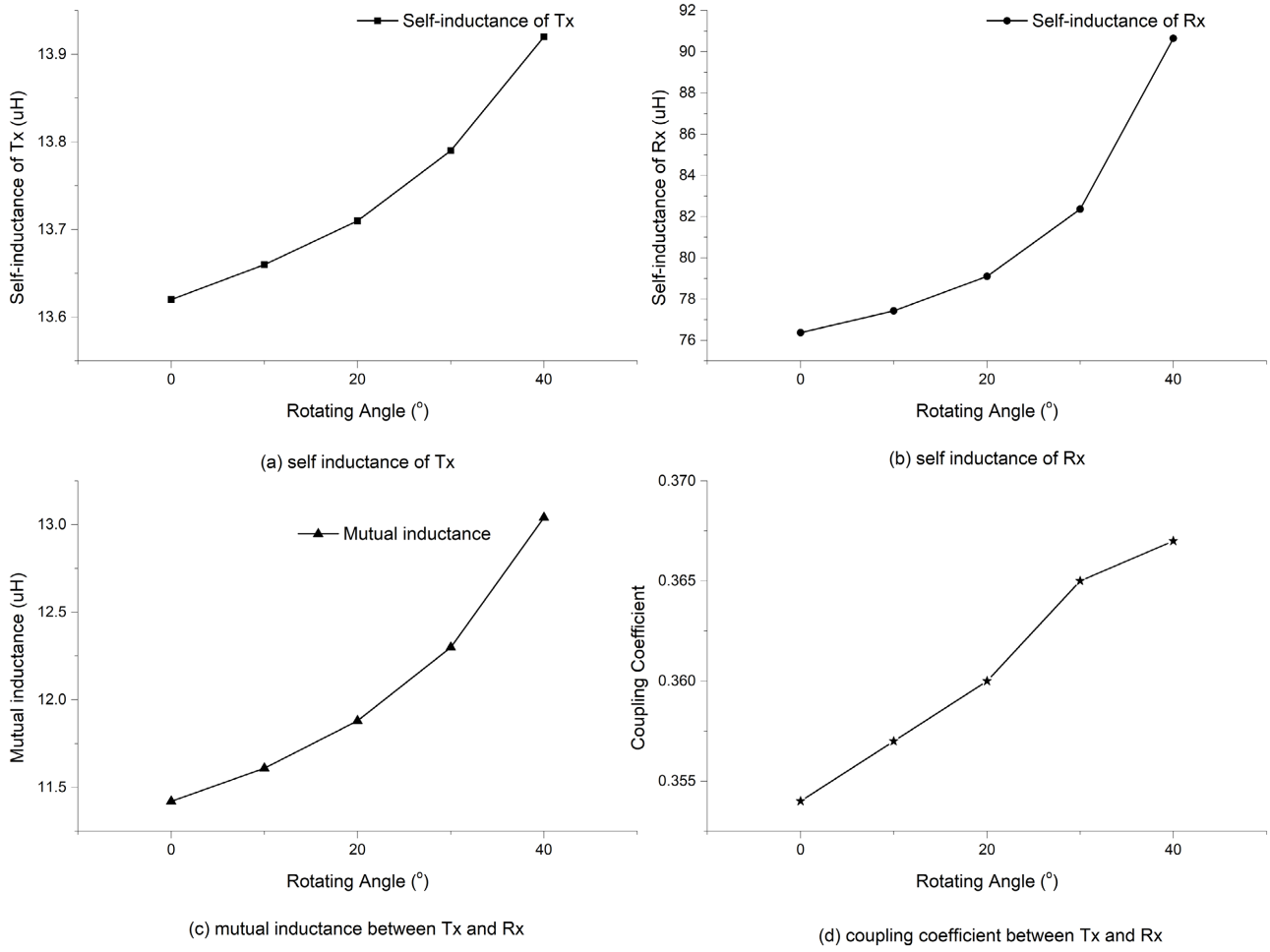

Figure 6. Self-inductance of (a) Tx, (b) Rx, (c) mutual inductance, and (d) coupling coefficient against rotating angle.

3.2. Coupling Performance Comparison of Proposed Design with Three Typical Designs via Maxwell

In order to evaluate the function of power repeaters in the proposed system, three typical designs are considered. Those designs were simulated under the same simulation setup in Maxwell as the proposed system in section A (listed above), including self-inductance of Tx and Rx coils, mutual inductance and coupling coefficient between Tx and Rx. Despite the proposed system simulated before, three different designs were considered from the Tx coil, Rx coil and power repeaters. As shown in Figure 7, (a) is the proposed system including a circular Tx coil with a ferrite sheet, two power repeaters that share the identical structure as the Tx coil, and a curved Rx coil that is designed as three square sub-coils with a curved ferrite sheet. Design in (b) removes power repeaters compared to (a), design in (c) replaces the Rx coil with a curved rectangular coil, and design in (d) replaces the Tx coil and power repeaters with a curved rectangular coil.

Figure 8 presented the comparison of simulated results of four designs mentioned above. First, for the proposed designs with/without power repeaters, it

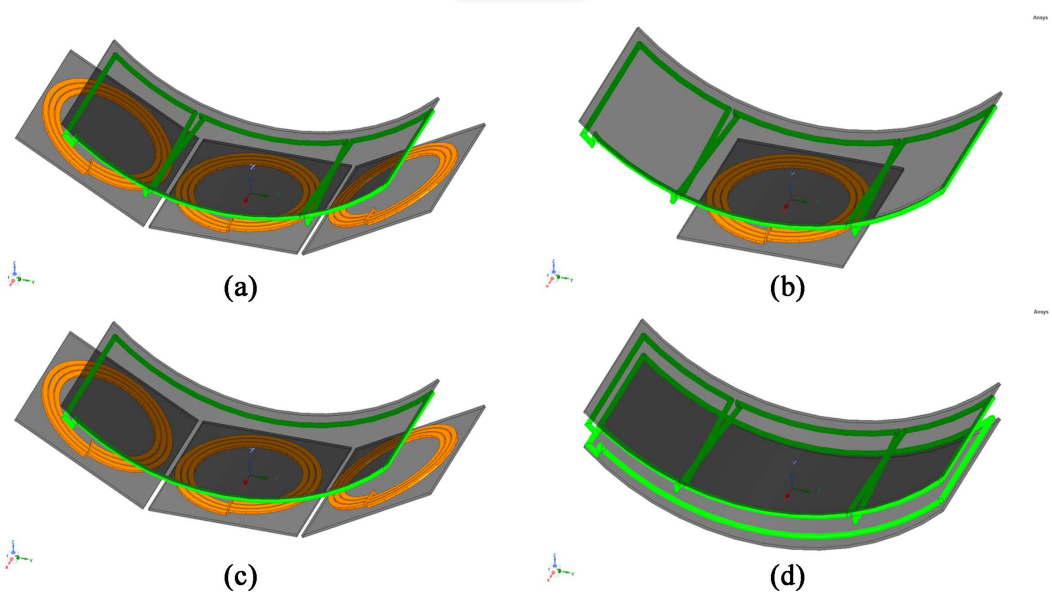

Figure 7. Different Tx/Rx coupling structures with and without power repeaters. (a) Proposed design; (b) Single Tx without repeaters; (c) Single curved rectangular Rx; (d) Single curved rectangular Tx.

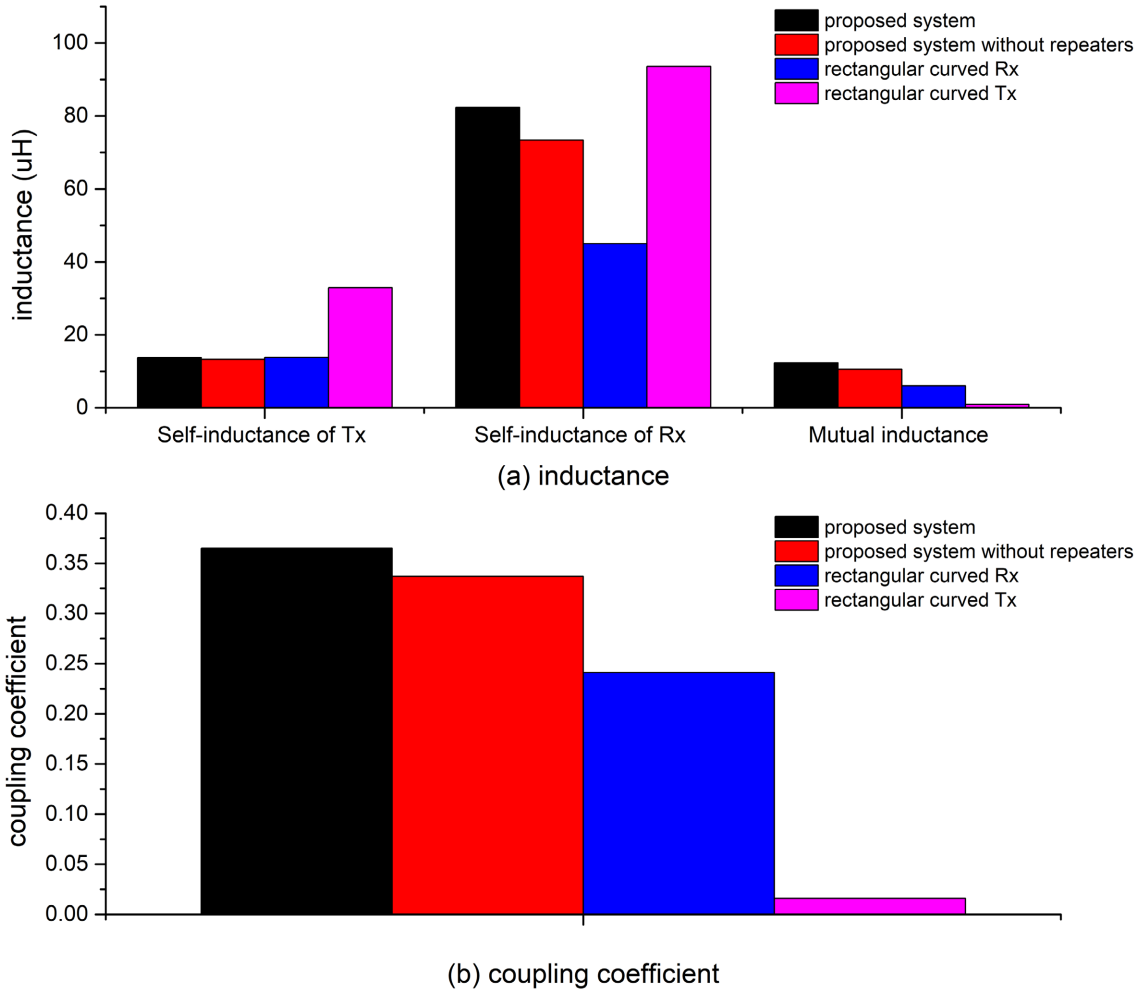

Figure 8. (a) Inductance and (b) coupling coefficient comparison of the proposed design with typical designs.

could be obtained that power repeaters could enhance the self-inductance of Rx and strengthen the coupling between Tx and Rx to some extent, besides, power repeaters may not influence the self-inductance of Tx coil. Next, if the Rx coil in proposed system was replaced with a curved rectangular coil in **Figure 7(c)**, both self-inductance of Rx and coupling coefficient would drop a little. Then, according to **Figure 8**, design in **Figure 7(d)** had the largest self-inductance of both Tx and Rx, but had the smallest mutual inductance, as well as coupling coefficient, which indicates this design may increase the self-inductance, but two coils may not couple well with each other. Compared to the circular coil design in **Figures 7(a)-(c)**, the model of curved rectangular Tx coil in simulation has less overlapping area facing to the Rx coil. This might be the reason of showing high self-inductance of Tx and Rx but a bad coupling performance.

3.3. Co-Simulation of Proposed System via Simplorer

Based on the self-inductance of both Tx and Rx coil and mutual inductance between them, further electrical simulation could also be conducted in Ansys Simplorer. This calculation was based on the self-inductance and the mutual inductance values already determined in the earlier stage (in Maxwell). As shown in **Figure 9**, for the first co-simulation, an uncompensated network was constructed with the same current supply, which guarantees the input current is 1A for both situations. The magnitude of V_{oc} and I_{sc} that could be obtained from **Figure 9** were 10.94 V and 0.21 A respectively. For uncompensated system, the power can be transferred at max power condition could be calculated by:

$$P_m = \frac{1}{2} V_{oc} I_{sc} \tag{8}$$

The value of P_m is 1.1 W under this condition. Moreover, V_{oc} and I_{sc} obtained from uncompensated network could also be used to predict how much power could be transferred with series compensation. As the self-inductance of the R_x coil L_s has been obtained in Maxwell which is 82.4 μH at 30˚, a 30.8 nF capacitor C_s connected in series with this inductor would make sure the system work at a fully tuned state. The power factor of the secondary side with a pure resistance R at 20 Ω can be obtained from:

$$Q_s = \frac{\omega_0 L_s}{R} \tag{9}$$

so the quality factor of the secondary side is 2.6, then the output power at a fully tuned state could be gained as:

$$P_m = Q_s V_{oc} I_{sc} \tag{10}$$

and the output power P_m is 6.0 W. Compared to 1.1 W under uncompensated state, adding tuning capacitors would hugely increase the power transferred through the proposed system.

For the second part of co-simulation, as shown in **Figure 3**, two capacitors C_p with 183.7 nF and C_s with 30.8 nF were added and connected in series with the Tx coil and the Rx coil respectively. A rated pure resistor with 20 Ω was also

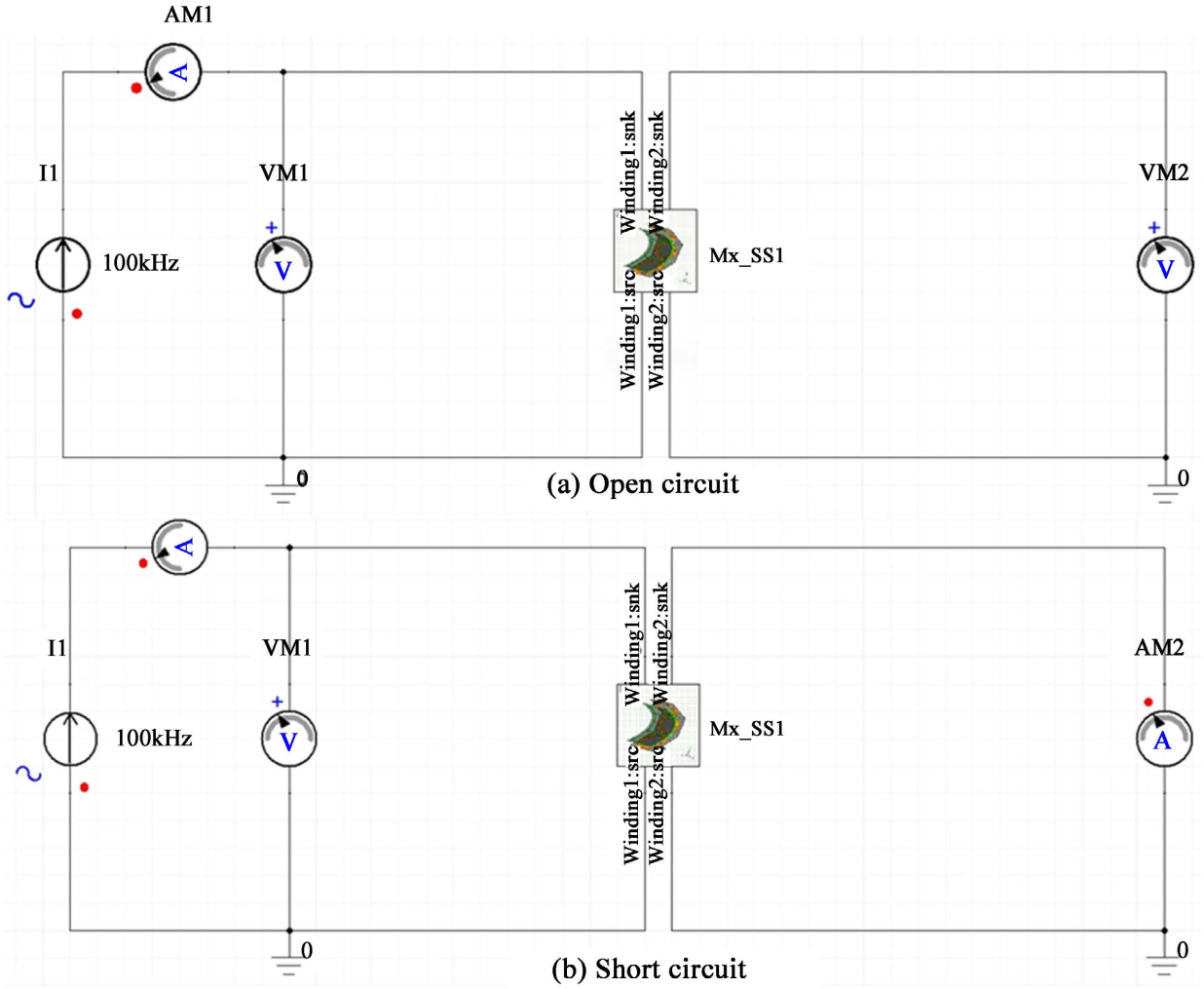

Figure 9. Schemes for Ansys Simplorer simulation.

Table 4. Comparison of calculated and simulated input and output power.

Inputs and Outputs	Calculated Results	Simulated Results
I_p (A)	3.31	3.34
I_s (A)	1.27	1.27
P_{in} (W)	32.6	33.2
P_{out} (W)	33.2	32.2

applied in the scheme. The power supply in this co-simulation is a 10 V voltage source at 100 kHz. Then, in Table 4, the input and output power calculated based on co-simulation currents and equivalent circuit theory in Part 2.2 were summarized. It could be seen that regardless of inner resistance of components in the circuit, the calculated results align well with the simulated results.

One point that should be emphasized again is that the inner resistance of wires, inductors and capacitors are ignored, so there is no extra loss through power transfer. Theoretically, the input power is supposed to equal to the output

power, as seen from Table 4. When considering the loss of components, two equivalent resistances should be added on the primary and secondary side respectively. Due to this, the input power may increase, but the output power may decrease and the difference between them is the power loss. In practical applications, this power loss may be demonstrated as heat in coils or circuits, which might reduce the power transfer efficiency or even break components with a high temperature. Also, part of energy may dissipate with the magnetic flux leakage in the air gap, which lowers down the power transfer efficiency.

3.4. Simulation of Full Bridge Rectifier on the Secondary via LTspice

To obtain a DC output on the secondary side which can charge a battery of a vacuum cleaner, a full bridge rectifier with filter capacitor was applied after the compensation capacitor on the secondary side in LTspice, as shown in Figure 10. The parameters in the system with power repeaters under 30˚ rotating angle was borrowed. Four Schottky diodes with 5 A average forward current and 150 V breakdown voltage were used to construct the bridge and a 3.75 μF. The filtering capacitor is paralleled with the load. The sinusoidal waveform of the output voltage and current without rectification is converted into nearly a ripple waveform. The output voltage across the load remained around 22.9 V and the output current through the load remained around 1.14 A, which could satisfy the charging standard of some commercial batteries of vacuum cleaners mentioned before. Under this circuit setup, the output power of the load decreased to about 26.0 W. It could also find that the output voltage and current might experience a longer time from start to a stable ripple output than the system without rectification in Part 3.3.

3.5. Evaluation of Power Transfer Performance

To evaluate the power transfer performance of the proposed wireless power transfer system, the power transfer to a 20-Ω rated load of two other typical magnetic designs with and without power repeaters shown in Figure 7(b) and

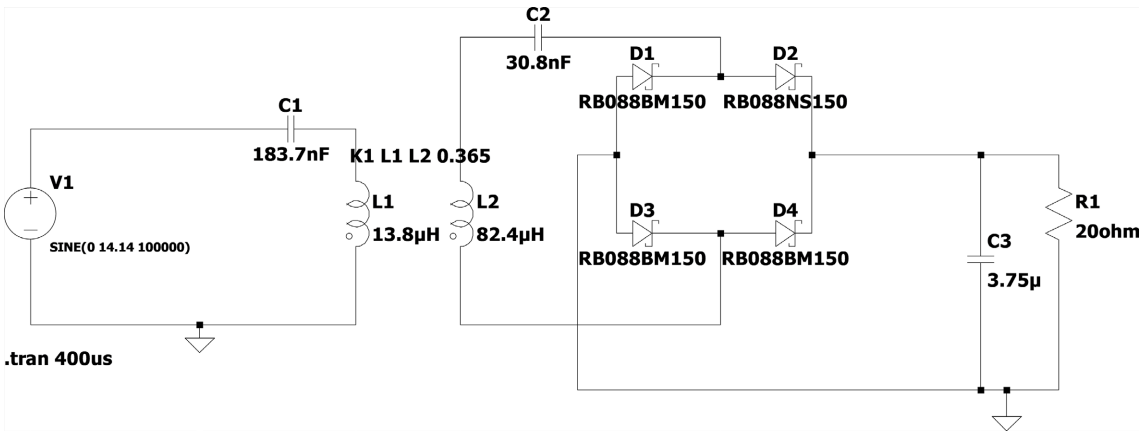

Figure 10. Scheme of the rectification network.

Figure 7(d) were studied. Option (c) in Figure 7 is not considered for comparison because it has a singular rectangular Rx which causes significant flux cancellation. The value of two tuning capacitors was selected to achieve full resonance of the design without power repeaters, and other two designs were simulated under the same circuit setup as the previous one, which means they were not working at full resonance state. The simulated output power of three designs was shown in Table 5.

It could be seen that the magnetic design without power repeaters would deliver the highest power among those designs, which is 33.8 W after rectification. When adding two proposed power repeaters to the circular Tx coil, the power delivery would decrease a little. During a small range of rotating angle from 0˚ to 20˚, the power delivery reduction would be about 1.5 W to 3.5 W, but it would reach about 5 W when the power repeater rotates more than 20˚. One possible reason for the power reduction is the power repeater in the proposed design could not achieve power transfer enhancement without tuning, even though it could enhance the coupling performance between the Tx coil and the Rx coil. Compared with other two designs, the design with a curved rectangular Tx coil could deliver about 26.0 W, which is the lowest power delivery among three designs. One conclusion drawn from above simulation results is that passive power repeaters could not enhance the power transfer capability but could change the coupling performance of the system. Things could be different when adding extra power supplies to power repeaters, the alternating magnetic fields generated by different sources may interact and the system may reach a resonant state where more power could be delivered.

In order to achieve the charging function in practical applications, further work on the conversion from commercial AC mains electricity to DC to high frequency AC before the primary compensation and regulation network after rectification should be continued. Furthermore, the coil design of Tx and Rx in this paper still have space to explore to achieve a better coupling performance and power transfer capability. Most important, the usage of power repeaters and the structure design of power repeaters are very limited in this paper, because the power repeater could also be activated by extra power supply to generate its own fields which might show some different features than the passive one when

Table 5. Comparison of simulated output power of different designs.

Magnetic Design	Simulated Output Power (W)
Proposed design at 0˚	32.3
Proposed design at 10˚	30.3
Proposed design at 20˚	31.0
Proposed design at 30˚	27.8
Proposed design without power repeaters	33.8
Curved rectangular Tx	26.0

it interacts with the magnetic field between Tx and Rx. This inherent magnetic field of the power repeaters may help with the possibility of artificial guidance to the magnetic field, even the power flow. For the passive power repeater, several methods, such as adding tuning capacitors to make it work at the same resonant frequency as the operating frequency of the system, and connecting power repeaters in series or in parallel, could be conducted to enhance both the coupling performance and the power delivery to load.

4. Conclusion

To conclude, in this paper, a wireless charger design of cylindrical robot vacuum cleaners with two adjustable power repeaters is proposed. This design aims to charge various vacuum cleaners of different sizes but with similar battery charging levels of around 20 W. The rotating function of the power repeater could make the charger system compatible with various curved Rx coils. The magnetic characteristics such as the self-inductance, mutual inductance and the coupling of the proposed magnetic design are simulated via FEM software, and three typical magnetic designs are also analyzed. The inductance of both coils and coupling performance between coils under different rotating angles are evaluated via simulation. The comparison results from those designs show that power repeaters could guide more magnetic flux to the Rx side and enhance the coupling between Tx and Rx to some extent. Next, an equivalent circuit of the proposed design under 30˚ is established with series-series tuning networks on both sides regardless of the inner resistance of components. After that, the primary current and output current is calculated to obtain the theoretical input and output power of the system under full-tuning conditions. Besides, co-simulation via Simplorer based on the magnetic simulation is conducted from two aspects. One is the uncompensated output power under a constant current source and the prediction of the output power with fully-tuned conditions. It is obvious that adding a compensation network would greatly increase the power transfer performance. The other co-simulation is based on a 20-ohm-rated resistance with series-series compensation. The current on both sides and power are obtained and they match well with the calculated results. The output power could reach around 32 W and this might be able to charge a battery in multiple kinds of vacuum cleaners safe and efficiently after further progress on conversion, rectification and coil design optimization. There is also room for further research on IPT systems with power repeaters and curved coils. For example, improving the tuning of high-order systems with passive power repeaters, or we can utilize the matrix configuration of repeaters. Active power repeaters may lead to a possibility of manipulating magnetic field distribution, and even power flow to achieve power transfer enhancement and orientation. The optimized magnetic design of curved coils might also enhance power transfer capability, which can be applied to a series of electronic devices and appliances.

Acknowledgements

The authors would like to acknowledge the help from two supervisors and the research group.

Conflicts of Interest

The authors declare no conflicts of interest regarding the publication of this paper.

References

[1] Zaheer, A., Covic, G.A. and Kacprzak, D. (2014) A Bipolar Pad in a 10-kHz 300-W Distributed IPT System for AGV Applications. *IEEE Transactions on Industrial Electronics*, **61**, 3288-3301. https://doi.org/10.1109/TIE.2013.2281167

[2] Jeong, S., Kim, D.-H., Song, J., Kim, H., Lee, S., Song, C., Lee, J., Song, J. and Kim, J. (2019) Smartwatch Strap Wireless Power Transfer System with Flexible PCB Coil and Shielding Material. *IEEE Transactions on Industrial Electronics*, **66**, 4054-4064. https://doi.org/10.1109/TIE.2018.2860534

[3] Tran, D.H., Vu, V.B. and Choi, W. (2018) Design of a High-Efficiency Wireless Power Transfer System with Intermediate Coils for the On-Board Chargers of Electric Vehicles. *IEEE Transactions on Power Electronics*, **33**, 175-187. https://doi.org/10.1109/TPEL.2017.2662067

[4] Bu, Y., Endo, S. and Mizuno, T. (2018) Improvement in the Transmission Efficiency of EV Wireless Power Transfer System Using a Magnetoplated Aluminum Pipe. *IEEE Transactions on Magnetics*, **54**, 1-5. https://doi.org/10.1109/TMAG.2018.2840109

[5] Campi, T., Cruciani, S., De Santis, V., Maradei, F. and Feliziani, M. (2018) Wireless Power Transfer (WPT) System for an Electric Vehicle (EV): How to Shield the Car from the Magnetic Field Generated by Two Planar Coils. *Wireless Power Transfer*, **5**, 1-8. https://doi.org/10.1017/wpt.2017.17

[6] Moon, S. and Moon, G.-W. (2016) Wireless Power Transfer System with an Asymmetric Four-Coil Resonator for Electric Vehicle Battery Chargers. *IEEE Transactions on Power Electronics*, **31**, 6844-6854.

[7] Wang, G., Liu, W., Sivaprakasam, M. and Kendir, G.A. (2005) Design and Analysis of an Adaptive Transcutaneous Power Telemetry for Biomedical Implants. *IEEE Transactions on Circuits and Systems I: Regular Papers*, **52**, 2109-2117. https://doi.org/10.1109/TCSI.2005.852923

[8] Gyu, B.J. and Cho, B.H. (1998) An Energy Transmission System for an Artificial Heart Using Leakage Inductance Compensation of Transcutaneous Transformer. *IEEE Transactions on Power Electronics*, **13**, 1013-1022. https://doi.org/10.1109/63.728328

[9] James, J.E.I., Chu, A., Robertson, D., Sabitov, A. and Covic, G.A. (2011) A Series Tuned High Power IPT Stage Lighting Controller. 2011 *IEEE Energy Conversion Congress and Exposition*, Phoenix, AZ, 17-22 September 2011, 2843-2849. https://doi.org/10.1109/ECCE.2011.6064151

[10] Yan, Z., Siyao, Q., Zhu, Q., Huang, L. and Hu, A.P. (2018) A Simple Brightness and Color Control Method for LED Lighting Based on Wireless Power Transfer. *IEEE Access*, **6**, 51477-51483. https://doi.org/10.1109/ACCESS.2018.2869883

[11] Lee, E.S., Sohn, Y.H., Choi, B.G., Han, S.H. and Rim, C.T. (2018) A Modularized

IPT with Magnetic Shielding for a Wide-Range Ubiquitous Wi-Power Zone. *IEEE Transactions on Power Electronics*, **33**, 9669-9690. https://doi.org/10.1109/TPEL.2017.2789201

[12] Lu, C., Rong, C., Huang, X., Hu, Z., Tao, X., Wang, S., Chen, J. and Liu, M. (2019) Investigation of Negative and Near-Zero Permeability Metamaterials for Increased Efficiency and Reduced Electromagnetic Field Leakage in a Wireless Power Transfer System. *IEEE Transactions on Electromagnetic Compatibility*, **61**, 1438-1446. https://doi.org/10.1109/TEMC.2018.2865520

[13] Zhong, W.X., Zhang, C., Liu, X. and Hui, S.Y.R. (2015) A Methodology for Making a Three-Coil Wireless Power Transfer System More Energy Efficient than a Two-Coil Counterpart for Extended Transfer Distance. *IEEE Transactions on Power Electronics*, **30**, 933-942. https://doi.org/10.1109/TPEL.2014.2312020

[14] Chen, Y., Mai, R., Zhang, Y., Li, M. and He, Z. (2019) Improving Misalignment Tolerance for IPT System Using a Third-Coil. *IEEE Transactions on Power Electronics*, **34**, 3009-3013. https://doi.org/10.1109/TPEL.2018.2867919

[15] Zhong, W.X., Liu, X. and Hui, S.Y.R. (2011) A Novel Single-Layer Winding Array and Receiver Coil Structure for Contactless Battery Charging Systems with Free-Positioning and Localized Charging Features. *IEEE Transactions on Industrial Electronics*, **58**, 4136-4144. https://doi.org/10.1109/TIE.2010.2098379

[16] Hua, R., Long, B. and Hu, A.P. (2017) Enhancing Wireless Power Transfer Capability of Inductive Power Transfer System Using Matrix Power Repeater. 2017 *IEEE 12th International Conference on Power Electronics and Drive Systems* (*PEDS*), 12-15 December 2017, Honolulu, HI, 957-961. https://doi.org/10.1109/PEDS.2017.8289259

[17] Hua, R. and Hu, A.P. (2019) Modeling and Analysis of Inductive Power Transfer System with Passive Matrix Power Repeater. *IEEE Transactions on Industrial Electronics*, **66**, 4406-4413. https://doi.org/10.1109/TIE.2018.2860560

[18] Hua, R., Kalra, G., Wang, V. and Hu, A.P. (2017) Extending the Inductive Power Transfer Range by Using Passive Power Repeaters. 2017 *12th IEEE Conference on Industrial Electronics and Applications* (*ICIEA*), Siem Reap, 18-20 June 2017, 1718-1722. https://doi.org/10.1109/ICIEA.2017.8283116

[19] Ying, H., Tianhuai, D. and Peng, W. (2013) Characteristics of Eddy Current Effects in Curved Flexible Coils. *Journal of Tsinghua University* (*Science and Technology*), **53**, 1429-1433.

[20] Burke, S.K., Ditchburn, R.J. and Theodoulidis, T.P. (2008) Impedance of Curved Rectangular Spiral Coils around a Conductive Cylinder. *Journal of Applied Physics*, **104**, Article ID: 014912. https://doi.org/10.1063/1.2951947

[21] Sandoval, F.S., Torres Delgado, S.M., Moazenzadeh, A. and Wallrabe, U. (2018) Flexible Wireless Power Transfer System Based on Closed-Loop Magnetoinductive Waveguides: Solution to Misaligned and Rotational Systems. *Journal of Physics: Conference Series*, **1052**, Article ID: 012077. https://doi.org/10.1088/1742-6596/1052/1/012077

[22] Daura, L.U., Tian, G., Yi, Q. and Sophian, A. (2020) Wireless Power Transfer-Based Eddy Current Non-Destructive Testing Using a Flexible Printed Coil Array. *Philosophical Transactions of the Royal Society A*: *Mathematical*, *Physical and Engineering Sciences*, **378**, Article ID: 20190579. https://doi.org/10.1098/rsta.2019.0579

[23] Wen, F., Jing, F., Li, Q., Li, R., Liu, L. and Chu, X. (2020) Curvature Angle Splitting Suppression and Optimization on Nonplanar Coils Used in Wireless Charging System. *IEEE Transactions on Power Electronics*, **35**, 9070-9081. https://doi.org/10.1109/TPEL.2020.2974619